J. Fluid Mech. (1979), *vol.* 94, *part* 1, *pp.* 1–12
Printed in Great Britain

The round laminar jet in a spherical envelope

By W. M. PICKERING AND C. SOZOU
Department of Applied Mathematics and Computing Science,
University of Sheffield, England

(Received 18 December 1978)

A nonlinear solution is constructed representing the steady flow field generated in viscous incompressible fluid in a spherical envelope by a constant point force F_0 acting at the centre O of the envelope. Our analysis shows that when $F_0 = O(3\nu^2\rho)$, where ν is the coefficient of kinematic viscosity and ρ the density of the fluid, the linear solution, which is symmetric about a plane through O perpendicular to the force, represents a reasonable approximation to the velocity field. As F_0 increases the velocity field develops an asymmetry and the centre of the eddy, that exists in a meridian section, is displaced towards the direction of the force and is closer to the boundary. Also as F_0 increases, on the axis of symmetry, the fluid speed per unit force decreases behind the force and increases ahead of it and percentage-wise the increase is larger further from O.

1. Introduction

The stokeslet – that is, the steady-state linear flow field generated by a point force – has been studied for some time now with various boundary conditions; numerous references and applications of this in the biological field can be found in a review article by Lighthill (1976). More recently Liron & Shahar (1978) investigated the flow field induced by a point force in an infinitely long circular pipe. The basic approach for tackling the linear problem is straightforward, though the algebra could be complicated. The solution consists of two parts, that is the basic solution representing the stokeslet plus another component which is finite throughout the region of interest and takes prescribed values on the boundary so that the total velocity is zero there.

There are not many solutions representing nonlinear flow fields generated by a point force. There is, in effect, only the solution representing the classical Landau–Squire momentum jet, that is the steady flow field generated by a point force in an infinite fluid. The development of this momentum jet was recently considered by Sozou & Pickering (1977). There is also Squire's (1952) momentum jet representing the flow field generated by a point force acting through a small hole in a plate bounding a semi-infinite fluid, the force being perpendicular to the plate and pointing into the fluid, but there are doubts about the physical interpretation of Squire's solution. The tangential velocity on the plate is not zero and the solution is not unique, that is this force can produce an inflow from the region adjacent to the plate and, along the direction of the force, a discharge perpendicular to the plane, but as pointed out by Sozou (1971) the reverse picture (momentum sink) is also compatible with this force. Also, on similarity grounds the velocity field of Squire's solution is proportional to r^{-1}, where r is the distance from the force, but recently Blake (1971) showed that, in the linear regime, the far flow field generated by a force perpendicular to the plate and at a distance a from it is proportional to r^{-3}.

0022-1120/79/4307-7330 $02.00

The importance of the momentum jets was recently emphasized by Lighthill (1978, § 4.7), who suggested that in ultrasonics the attenuated energy of an acoustic beam generates a mean force that drives a velocity field known as the 'sonic' wind. For low power output the stokeslet represents an adequate representation of the flow field generated but when the power output of the beam is large the sonic wind field near the source of the force, where boundaries are unimportant, resembles that of the Landau–Squire jet. This momentum jet clearly demonstrates that the streamline pattern is not symmetrical about a plane through the point of application of the force which is perpendicular to the axis (direction) of the force in contradistinction to the corresponding linear problem. On the axis of the jet, for instance, ahead of the force the flow field is stronger and behind it weaker than that associated with the stokeslet and this asymmetry increases as the magnitude of the applied force increases. The presence of boundaries must influence the nonlinearities of the problem, especially close to them, and it would be of interest to construct nonlinear solutions in order to study the effect of boundaries. The solution of the nonlinear problem, however, in the presence of general boundaries presents great difficulties as pointed out by Lighthill (1978), but in some special cases it may be possible to construct numerical solutions. We note that the Landau–Squire solution was constructed by means of similarity principles, the argument being that, since there are no explicit scale lengths present, the stream function ψ associated with the flow field must, on dimensional grounds, be of the form $\psi = \nu r g_0(\mu)$, where ν is the coefficient of kinematic viscosity of the fluid, r the distance from the force and $\mu = \cos\theta$, θ being the angle between the direction of the force and the radial vector from the force to the test point. When the flow field has axial symmetry and the boundary does not pass through the point of application of the force we can attempt to construct a nonlinear solution by setting $\psi = \nu r g$, g being a function of μ and r that satisfies the condition $g \sim g_0$ as $r \to 0$. The solution of the resulting equations could be a formidable problem, even numerically, depending on the shape of the boundary. Perhaps the simplest case arises in the extension of the problem considered in Lamb's (1962, p. 606) *Hydrodynamics*, that is, the flow field due to a force at the centre of a fluid bounded by a spherical envelope, to the nonlinear regime. This we undertake below.

2. Formulation of the problem

We consider a spherical envelope of radius a containing viscous incompressible fluid. We shall denote the pressure, coefficient of kinematic viscosity and density of the fluid by p, ν and ρ, respectively. The fluid is acted on by a constant force F_0 at the origin O along the direction $\theta = 0$ of a spherical polar co-ordinate system (r, θ, ϕ), O coinciding with the centre of the cavity. The velocity field $\mathbf{v}$ will clearly be symmetric about the axis $\theta = 0, \pi$ and, it is convenient to express the steady-state form of the stream function ψ associated with $\mathbf{v}$ by

$$\psi = \nu r g(\mu, R) \tag{1}$$

where $\mu = \cos\theta$ and $R = r/a$. Thus the spherical container corresponds to $R = 1$. Now

$$\mathbf{v} = -\nu r^{-1}[g_\mu, (g + R g_R)/(1-\mu^2)^{\frac{1}{2}}, 0], \tag{2}$$

where a suffix μ or R denotes partial differentiation with respect to that variable. On taking the curl of the steady-state momentum equation

$$\mathbf{v}.\nabla\mathbf{v} = -\frac{1}{\rho}\nabla p + \nu\nabla^2\mathbf{v} \tag{3}$$

and making use of (2), after a little algebra, we obtain

$$(1-\mu^2)f_{\mu\mu} - 4\mu f_\mu + R^2 f_{RR} - 2Rf_R = 3fg_\mu + gf_\mu + R(f_\mu g_R - f_R g_\mu), \tag{4}$$

where

$$f = g_{\mu\mu} + (2Rg_R + R^2 g_{RR})/(1-\mu^2). \tag{5}$$

The function f and the fluid vorticity $\nabla\times\mathbf{v}$ are connected by

$$\nabla\times\mathbf{v} = [0, 0, -\nu(1-\mu^2)^{\frac{1}{2}} r^{-2} f]. \tag{6}$$

Equations (4) and (5) are the fundamental equations of our problem. For $r \ll a$, that is as $R \to 0$, $g(\mu, R) \sim g_0(\mu)$ and equation (5) becomes $f = f_0(\mu) = g_0''$; then (4) reduces to

$$(1-\mu^2)g_0^{\mathrm{iv}} - 4\mu g_0''' = 3g_0' g_0'' + gg_0'''. \tag{7}$$

The solution of (7) is well known and the appropriate functions f_0 and g_0 that make $\mathbf{v}$ finite on $\mu = \pm 1$ are given by

$$f_0 = -4c(c+2)/(1+c-\mu)^3, \tag{8}$$

$$g_0 = 2(1-\mu^2)/(1+c-\mu), \tag{9}$$

where $c(>0)$ is a parameter that is related to the impressed force which generates the flow field (Batchelor 1967, p. 207) by the equation:

$$\frac{F_0}{2\pi\nu^2\rho} = \frac{32}{3}\frac{1+c}{c(2+c)} + 4(1+c)^2\log\left(\frac{c}{c+2}\right) + 8(1+c). \tag{10}$$

Large values of c correspond to small values of F_0 and small values of c correspond to large F_0.

Equations (4) and (5) must be solved, in the region $0 \leqslant R \leqslant 1$, $-1 \leqslant \mu \leqslant 1$, subject to the following boundary conditions:

$$f(\mu, 0) = g_0'', \quad g(\mu, 0) = g_0, \tag{11), (12}$$

$$g(\mu, 1) = 0, \quad g_R(\mu, 1) = 0, \quad g(\pm 1, R) = 0, \tag{13)–(16}$$

$$\mp 4f_\mu + R^2 f_{RR} - 2Rf_R = 3fg_\mu - Rf_R\, g_\mu = 0 \quad \text{on} \quad \mu = \pm 1. \tag{17), (18}$$

Equations (13) and (14) imply that $\mathbf{v} = 0$ on the spherical boundary.
Equations (15) and (16) imply that $\mathbf{v}$ is finite on $\mu = \pm 1$, and (17) and (18) imply that $f_{\mu\mu}$ is finite on $\mu = \pm 1$.

By integrating the transverse component of (3) we find that

$$p = \nu^2\rho r^{-2} h(\mu, R), \tag{19}$$

where

$$h = -\frac{1}{2}\left[g_\mu^2 + \frac{(g+Rg_R)^2}{1-\mu^2}\right] + \int_0^\mu (fg_\mu - f + Rf_R)\,d\mu + h_0(R). \tag{20}$$

The total force acting on the fluid within a closed surface S is equal to the momentum

flux out of S. Taking for S the surface of a sphere of radius r_0 surrounding the origin, we obtain

$$F_0 + 2\pi r_0^2 \int_{-1}^{1} [\mu\sigma_{rr} - (1-\mu^2)^{\frac{1}{2}}\sigma_{r\theta}]\,d\mu = 2\pi r_0^2 \int_{-1}^{1} \rho \mathbf{v}.\hat{\mathbf{r}}(\mu \mathbf{v}.\hat{\mathbf{r}} - (1-\mu^2)^{\frac{1}{2}}\mathbf{v}.\hat{\boldsymbol{\theta}})\,d\mu, \quad (21)$$

where

$$2\pi r_0^2 \int_{-1}^{1} [\mu\sigma_{rr} - (1-\mu^2)^{\frac{1}{2}}\sigma_{r\theta}]\,d\mu$$

represents the force exerted by the surrounding fluid on S in the direction of F_0 and

$$\sigma_{rr} = -p + 2\nu\rho \frac{\partial}{\partial r}(\mathbf{v}.\hat{\mathbf{r}}), \quad \sigma_{r\theta} = \nu\rho\left[r\frac{\partial}{\partial r}\left(\frac{\mathbf{v}.\hat{\boldsymbol{\theta}}}{r}\right) + \frac{1}{r}\frac{\partial}{\partial\theta}(\mathbf{v}.\hat{\mathbf{r}})\right]. \quad (22), (23)$$

On substituting the expressions for σ_{rr}, $\sigma_{r\theta}$ and $\mathbf{v}$ in (21), after some algebra and integration of part of the resulting expression, we establish the equation

$$\frac{F_0}{2\pi\nu^2\rho} = \int_{-1}^{1} [\mu(h+g_\mu^2) - Rg_R\, g_\mu - R^2 g_{RR} + 2g - 2Rg_R]\,d\mu. \quad (24)$$

The right-hand side of (24) must be a constant for all R satisfying the condition $1 \geqslant R \geqslant 0$. If we set $R = 0, g = g_0, f = g_0''$ we can show that the right-hand side of (24) can be reduced to that of (10). Equation (24) can be used as an indication of the accuracy of the numerical solution we shall construct. If our solution is accurate (24) must be in reasonably good agreement with (10) for all values of R in the range of interest.

3. The linearized problem

The solution of the linear problem was constructed by Lamb (p. 606) in Cartesian co-ordinates. It is, however, instructive to construct a linearized solution of (4) and (5) in spherical polars. For large c equations (8) and (9) may be expanded in powers of $1/(c+1)$, that is

$$f_0 = -\frac{4}{(c+1)} - \frac{12\mu}{(c+1)^2} - \frac{4}{5(c+1)^3}(1 + 6(5\mu^2-1)) + \ldots, \quad (25)$$

$$g_0 = (1-\mu^2)\left[\frac{2}{c+1} + \frac{2\mu}{(c+1)^2} + \frac{2}{5(c+1)^3}(1 + (5\mu^2-1)) + \ldots\right]. \quad (26)$$

The powers of μ in (25) and in the square brackets in (26) have been expressed as derivatives of Legendre polynomials. Equations (25) and (26) suggest that we set

$$f = \frac{1}{c+1}f_1 + \frac{\mu}{(c+1)^2}f_2 + \frac{1}{(c+1)^3}(f_3^0 + (5\mu^2-1)f_3^1) + \ldots, \quad (27)$$

$$g = (1-\mu^2)\left[\frac{g_1}{c+1} + \frac{\mu}{(c+1)^2}g_2 + \frac{1}{(c+1)^3}(g_3^0 + (5\mu^2-1)g_3^1) + \ldots\right], \quad (28)$$

where $f_1, f_2, \ldots, g_3^1$ are functions of R. When we substitute (27) and (28) in (4) and (5) and equate the coefficients of $1/(c+1)$, $1/(c+1)^2$ and $1/(c+1)^3$ on the two sides of the resulting equation we obtain a set of equations involving $f_1, f_2, \ldots, g_3^1$. This set can be solved hierarchically, that is for f_1 and g_1 for a solution which is accurate to order $1/(c+1)$, then for f_2 and g_2 for accuracy to order $1/(c+1)^2$ and so on. The procedure is

straightforward and the solutions that make $\mathbf{v} = 0$ on $R = 1$ and reduce to (25) and (26) at $R = 0$ are

$$f_1 = -4 + 10R^3, \quad g_1 = 2 - 3R + R^3, \tag{29), (30}$$

$$f_2 = -12 + 12R - 6R^3 + 14R^4, \quad g_2 = 2 - 3R + R^2 - R^3 + R^4, \tag{31), (32}$$

$$f_3^0 = \tfrac{1}{5}[-4 - 72R + 84R^2 - 48R^3 \log R - \tfrac{694}{15}R^3 + 108R^4 - 42R^5 - \tfrac{16}{3}R^6 + 9R^7], \tag{33}$$

$$g_3^0 = \tfrac{1}{5}[2 - \tfrac{394}{15}R - 24R \log R + 21R^2 - \tfrac{19}{15}R^3 - \tfrac{24}{5}R^3 \log R + 6R^4 - \tfrac{3}{2}R^5 - \tfrac{2}{15}R^6 + \tfrac{1}{6}R^7], \tag{34}$$

$$f_3^1 = \tfrac{1}{5}[-24 + 43R - 21R^2 - \tfrac{48}{5}R^3 + \tfrac{34}{3}R^4 + \tfrac{1220}{77}R^5 + 3R^6 - \tfrac{14}{9}R^7], \tag{35}$$

$$g_3^1 = \tfrac{2}{5} - \tfrac{43}{50}R + \tfrac{21}{20}R^2 - \tfrac{24}{175}R^3 \log R - \tfrac{3680909}{3465050}R^3 + \tfrac{17}{60}R^4 + \tfrac{1223}{693}R^5 + \tfrac{1}{50}R^6 - \tfrac{7}{990}R^7. \tag{36}$$

From (10) we obtain [for $1 \gg 1/(c+1)$]

$$\frac{F_0}{16\pi\nu^2\rho} = \frac{1}{c+1} + \frac{17}{15}\frac{1}{(c+1)^3} + \ldots, \tag{37}$$

and this expansion converges for $c > 0$.

Lamb's linear solution is obtained by retaining only terms of order $1/(c+1)$, that is by setting

$$F_0/(16\pi\nu^2\rho) = 1/(c+1), \quad f = f_1/(c+1), \quad g = (1-\mu^2)\,g_1/(c+1)$$

and eliminating c between these equations.

It is clear from (27)–(37) that the linear solution represents a reasonable approximation to the g field when $F_0 = O(3\nu^2\rho)$, that is when $c = O(15)$ but in order to represent the f field by $f_1/(c+1)$ to the same degree of accuracy c must be 3 times as large. If, however, we retain terms to order $1/(c+1)^2$ the approximation of f and g is reasonably accurate when $c = O(10)$ or $F_0 = O(6\nu^2\rho)$. When $c = 5$ the values of $F_0/\nu^2\rho$ obtained from (37) to order $1/(c+1)^3$ and from the complete expression (10) are 8·64 and 8·65 and this suggests that when $F_0 = O(10\nu^2\rho)$ our third-order approximation will be in close agreement with the full solution. This we confirmed by comparing the third-order approximation with our numerical solution (see §5).

4. The numerical method

Equations (4) and (5) are elliptic within the region $-1 < \mu < 1$, $0 < R < 1$, but become parabolic on the boundaries $\mu = \pm 1$ and $R = 0$. It is convenient to transform into equations which are elliptic throughout the region of interest; for this we follow Sozou & Pickering (1977) and set

$$\eta = 1 - (1-\mu)^{\frac{1}{2}}, \qquad 0 \leqslant \mu \leqslant 1, \tag{38a}$$

$$\eta = (1+\mu)^{\frac{1}{2}} - 1, \quad -1 \leqslant \mu \leqslant 0, \tag{38b}$$

$$\xi = \log R, \tag{39}$$

and

$$f(\mu, R) = F(\eta, \xi), \quad g(\mu, R) = G(\eta, \xi).$$

Hence, equations (4) and (5) become

$$(1 + 2\eta - \eta^2)\,F_{\eta\eta} - (2G + 2G_\xi + 14\eta - 7\eta^2 - 1)\,F_\eta/(1-\eta) + 4F_{\xi\xi} + 2[G_\eta/(1-\eta) - 6]\,F_\xi - 6FG_\eta/(1-\eta) = 0, \tag{40a}$$

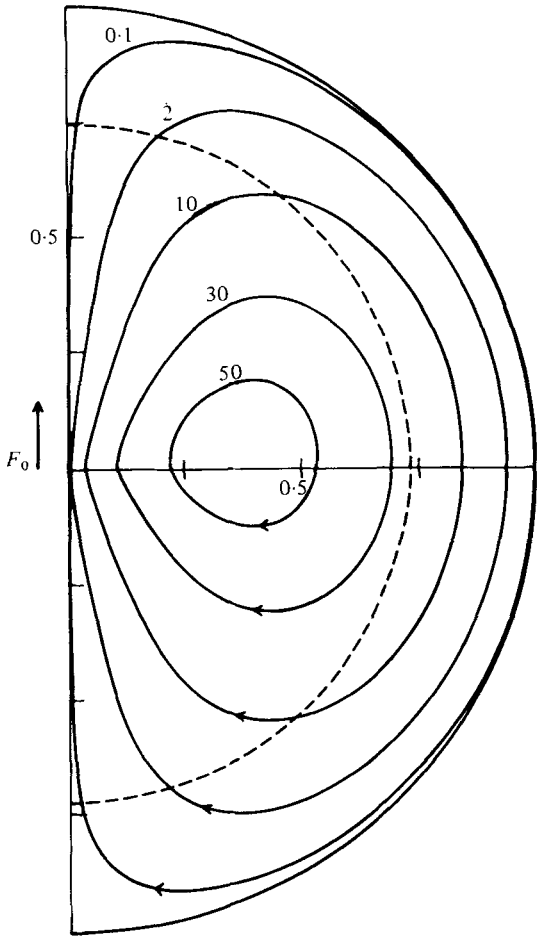

FIGURE 1. Streamline pattern in a meridian plane for the case $c = 5$ or $F_0 = 8{\cdot}65\nu^2\rho$. The numbers on the curves are values of $1000\psi/\nu a$. The vorticity within the region bounded by the broken curve is directed in the positive ϕ direction and in the surrounding region it is directed in the opposite sense.

$$(1-2\eta-\eta^2)F_{\eta\eta} - (2G + 2G_\xi + 14\eta + 7\eta^2 + 1)F_\eta/(1+\eta) + 4F_{\xi\xi} + 2[G_\eta/(1+\eta) - 6]F_\xi - 6FG_\eta/(1-\eta) = 0, \tag{40b}$$

$$(1+2\eta-\eta^2)[G_{\eta\eta} + G_\eta/(1-\eta)] + 4(G_{\xi\xi} + G_\xi) = 4F(1-\eta)^2(1+2\eta-\eta^2), \tag{41a}$$

$$(1-2\eta-\eta^2)[G_{\eta\eta} - G_\eta/(1+\eta)] + 4(G_{\xi\xi} + G_\xi) = 4F(1+\eta)^2(1-2\eta-\eta^2). \tag{41b}$$

Equations (40a) and (41a) hold for $0 \leqslant \eta \leqslant 1$ whereas (40b) and (41b) hold for $-1 \leqslant \eta \leqslant 0$. On $\mu = \eta = 0$, equations (40) reduce to the corresponding form of (4) and similarly (41) reduce to (5). For the equations on $\mu = 0$ we used (4) and (5) and set $\delta\mu = \delta\eta(2-\delta\eta)$. We note that the transformation used makes $R = 0$ correspond to $\xi = -\infty$ and $R = 1$ correspond to $\xi = 0$, that is the region of interest in the ξ, η plane is a semi-infinite strip. In order to reduce the length of the strip we make the reasonable

assumption that the solution at $R = R_0$, where $R_0 \ll 1$, may be approximated by the known solution at $R = 0$ and thus perform our computations in the finite strip

$$\xi_0 \leqslant \xi \leqslant 0, \quad -1 \leqslant \eta \leqslant 1,$$

where $\xi_0 = \log R_0$. In the actual calculations we set $R_0 = 0{\cdot}01$ and so $\xi_0 \approx -4{\cdot}61$. The boundary conditions (11)–(16) are now transformed to

$$F(\eta, \xi_0) = g_0''(\mu), \quad G(\eta, \xi_0) = g_0(\mu), \tag{42), (43}$$

$$G(\eta, 0) = 0, \quad G_\xi(\eta, 0) = 0, \quad G(\pm 1, \xi) = 0 \tag{44)–(47}$$

and equations (17) and (18), that express the condition that $f_{\mu\mu}$ is finite on $\mu = \pm 1$, were replaced by the equations

$$F_\eta(\pm 1, \xi) = 0 \tag{48), (49}$$

together with the requirement that, as $\eta \to 1$,

$$F_\eta/(1-\eta) = -F_{\eta\eta}, \quad G_\eta/(1-\eta) = -G_{\eta\eta} \tag{50), (51}$$

and as $\eta \to -1$

$$F_\eta/(1+\eta) = F_{\eta\eta}, \quad G_\eta/(1+\eta) = G_{\eta\eta}. \tag{52), (53}$$

We note that on $\xi = 0$ F can be determined in terms of G from (41a, b), (44) and (45) in the form

$$F = G_{\xi\xi}(\eta, 0)/[(1-\eta)^2(1+2\eta-\eta^2)] \quad \text{for} \quad 0 \leqslant \eta \leqslant 1. \tag{54a}$$

and

$$F = G_{\xi\xi}(\eta, 0)/[(1+\eta)^2(1-2\eta-\eta^2)] \quad \text{for} \quad -1 \leqslant \eta \leqslant 0. \tag{54b}$$

Thus if G is known we can solve (40a, b) for F subject to (42), (48), (49) and (54a, b). Similarly if F is known (41a, b) can be solved for G subject to (43), (44), (46) and (47).

We note that if we approximate G_ξ by second-order differences (44) and (45) imply

$$4G(\eta, -\delta\xi) = G(\eta, -2\delta\xi), \tag{55}$$

where $\delta\xi(>0)$ is the steplength in the ξ direction. Hence in order to incorporate explicitly (45) in the solution we constructed, we solved (41a, b) for G in the region $-1 < \eta < 1$, $\xi_0 < \xi < -\delta\xi$ subject to (43), (46), (47) and (55).

The numerical techniques used to express (40) and (41) in finite difference form were very similar to those employed previously (Sozou & Pickering 1975). The equations for F (40a, b) were solved iteratively using successive over-relaxation and those for G (41a, b) directly using the fast Fourier transform method [see, for example, Le Bail (1972)]. The Fourier transform was employed in the ξ direction.

The overall solution process was as follows. We specified an initial approximation to G, and, using a second-order approximation for $G_{\xi\xi}$, estimated $F(\eta, 0)$ from (54a, b) and solved (40a, b) for F. Equations (41a, b) were then solved for G and equation (55) was used to recalculate $G(\eta, -\delta\xi)$. Equations (54a, b) were again used to obtain improved estimates of $F(\eta, 0) = G_{\xi\xi}$ which were used to construct an improved approximation for F. The new F was used for an improved solution for G and so on until convergence. Convergence was assumed when two successive iterations produced changes of less than 0·1 % in both F and G at all mesh points. In the calculation of (54a, b) and (55) we employed under-relaxation. The mesh lengths in the ξ and η directions were $-\xi_0/257 \simeq 0{\cdot}018$ and $\frac{1}{11}$, respectively.

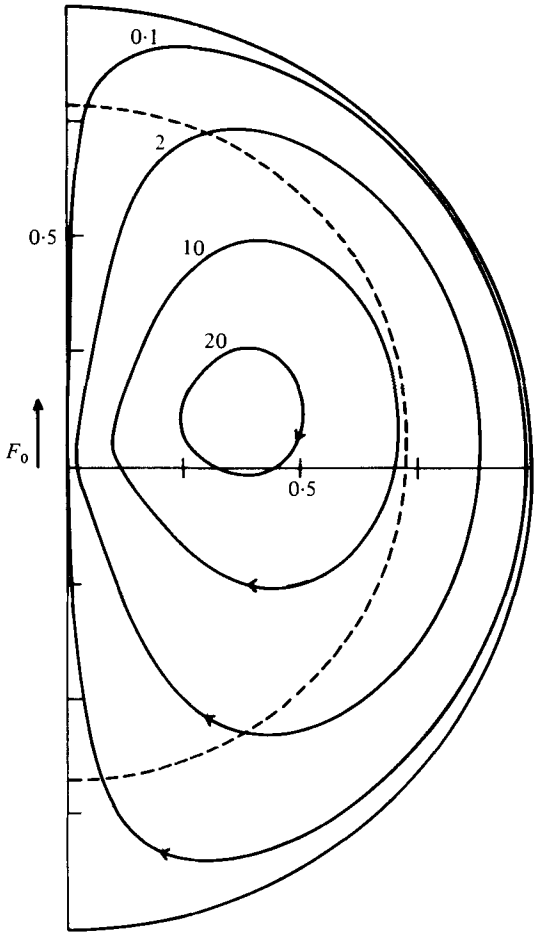

FIGURE 2. Streamline pattern in a meridian plane for the case $c = 1$ or $F_0 = 34{\cdot}77\nu^2\rho$. The numbers on the curves are values of $100\psi/\nu a$. The vorticity within the region bounded by the broken curve is directed in the positive ϕ direction and in the surrounding region it is directed in the opposite sense.

5. Results and discussion

We have computed the solutions for the cases $c = 5$, 1 and 0·2. The corresponding values of $F_0/\nu^2\rho$ are 8·65, 34·77 and 156·32. Streamlines of the respective flow fields are shown in figures 1–3. When $c = 5$ the problem is weakly nonlinear and the solution we constructed, starting from (27) and (28) to order $1/(c+1)^3$ as an initial approximation, converged very rapidly. Indeed the computed f and g fields hardly differed from those corresponding to the approximations (27) and (28) except near the boundary $R = 1$. Near $R = 1$ the maximum discrepancy between the computed solution and that given by (27) and (28) occurred in the g field, the computed g being about 7 % smaller than that given by (28). As c decreases the nonlinearities become more pronounced, though down to $c = 0{\cdot}2$ the construction of the solution was not particularly difficult. For values of $c \ll 0{\cdot}2$ the spatial variation of f is very rapid and it becomes rather difficult

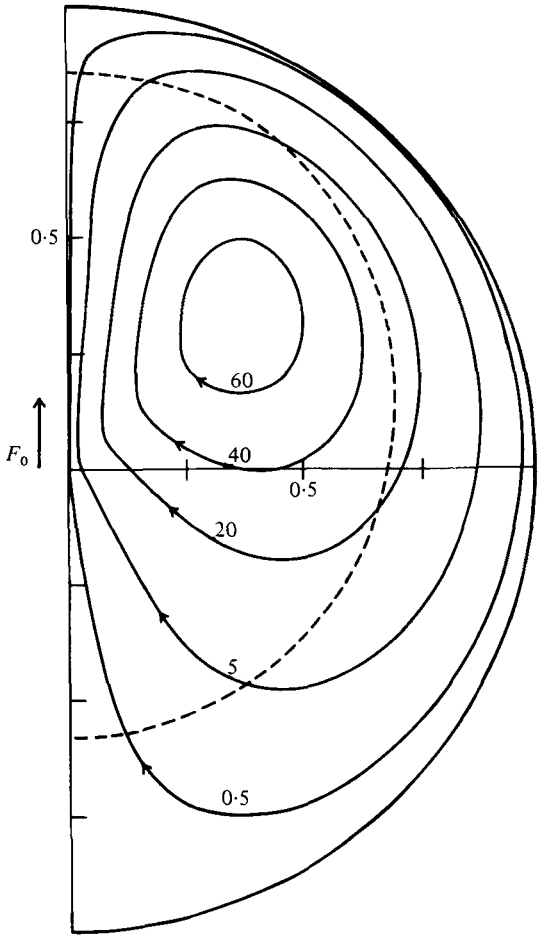

FIGURE 3. Streamline pattern in a meridian plane for the case $c = 0{\cdot}2$ or $F_0 = 156{\cdot}32\nu^2\rho$. The numbers on the curves are values of $100\psi/\nu a$. The vorticity within the region bounded by the broken curve is directed in the positive ϕ direction and in the surrounding region it is directed in the opposite sense.

to construct a convergent solution. We believe, however, that the values of c considered here bring out all the essential features of the nonlinear flow fields.

As suggested in § 2 an indication of the accuracy of our numerical solution can be obtained by checking for the satisfaction of (24) at all values of R. Our computations, using second-order differences for the derivatives and Simpson's rule for integration, have shown that the right-hand side of (24) is approximately a constant whose value is given by (10). For the case $c = 5$ and $c = 1$ the computed value of the right-hand side of (24) differed by less than 2·5 % from its expected constant value for all $R < 0{\cdot}7$. For larger values of R the discrepancy between (10) and (24) got progressively worse and near the boundary $R = 1$ it was just under 7 %. For the case $c = 0{\cdot}2$ the discrepancy between (10) and (24) was a little worse and its maximum value, occurring close to $R = 1$, was about 10 %. Since, however, the problem for the case $c = 0{\cdot}2$ is highly nonlinear we believe that the computed solution is reasonably accurate for all three values of c we used.

	c			
R	$\geqslant 100$ (linear case)	5	1	0·2
		$\mu = 1$		
0	7·96	9·25	11·50	12·72
0·2	5·60	6·70	9·67	13·23
0·4	3·44	4·14	6·53	12·11
0·6	1·66	2·01	3·38	8·87
0·8	0·45	0·55	0·97	3·43
		$\mu = -1$		
0	−7·96	−6·61	−3·84	−1·16
0·2	−5·60	−4·76	−2·86	−0·85
0·4	−3·44	−2·90	−1·73	−0·49
0·6	−1·66	−1·38	−0·80	−0·21
0·8	−0·45	−0·36	−0·20	−0·05
$F_0/(\nu^2\rho)$	$\ll 1$	8·65	34·77	156·32

TABLE 1. Values of $-100\nu^2\rho g_\mu/F_0$ on $\mu = \pm 1$ for some c and R

The linear flow field is symmetric about the plane $\mu = 0$ but the fields f_0 and g_0, that correspond to the Landau–Squire jet, are asymmetric. If for a specified c we define the asymmetry of these fields by $f_0(\mu)/f_0(-\mu)$ and $g_0(\mu)/g_0(-\mu)$ we find that their maximum asymmetry is given by

$$\frac{f_0(1)}{f_0(-1)} = \left(1+\frac{2}{c}\right)^3, \quad \frac{g_0(1)}{g_0(-1)} = 1+\frac{2}{c}$$

and thus unless c is exceedingly large one expects some asymmetry in the vorticity and velocity fields, especially the former. Our solution shows that away from the axial regions the asymmetry for the case $c = 5$ is reduced and the streamline pattern is not very asymmetric as can be confirmed by inspection of figure 1. This is to be expected, since for the case $c = 5$ the third-order solution represents a reasonable approximation and the asymmetry in the f and g fields is reflected in the second-order term which vanishes on $\mu = 0$.

As c decreases the nonlinearities of the problem become more intense. The asymmetry in the solutions f_0 and g_0 becomes more pronounced and the detailed data of our solution show that it also spreads throughout the fluid region. This is clearly demonstrated in the streamline pattern of figure 2, which represents the flow field for the case $c = 1$ and, even more so, in that of figure 3 which corresponds to the case $c = 0{\cdot}2$. From figures 1–3 it is deduced that when the value of c is decreased, that is F_0 is increased, the centre of the eddies is displaced from the plane $\mu = 0$ to larger values of μ and is further away from the force.

The radial velocity is $-2avg_\mu/R$ and values of $-100\nu^2\rho g_\mu/F_0$ along the axis $\mu = \pm 1$ for some c and R are shown in table 1. Inspection of this table shows that as F_0 increases the fluid speed per unit force increases on $\mu = 1$ and decreases on $\mu = -1$, and percentage-wise the increase (on $\mu = 1$) at a point P is larger the further P is from the origin. Also this table and detailed data of our output indicate that for any specified c percentage-wise the speed reduction per unit force on $\mu = -1$ as F_0 increases, diminishes

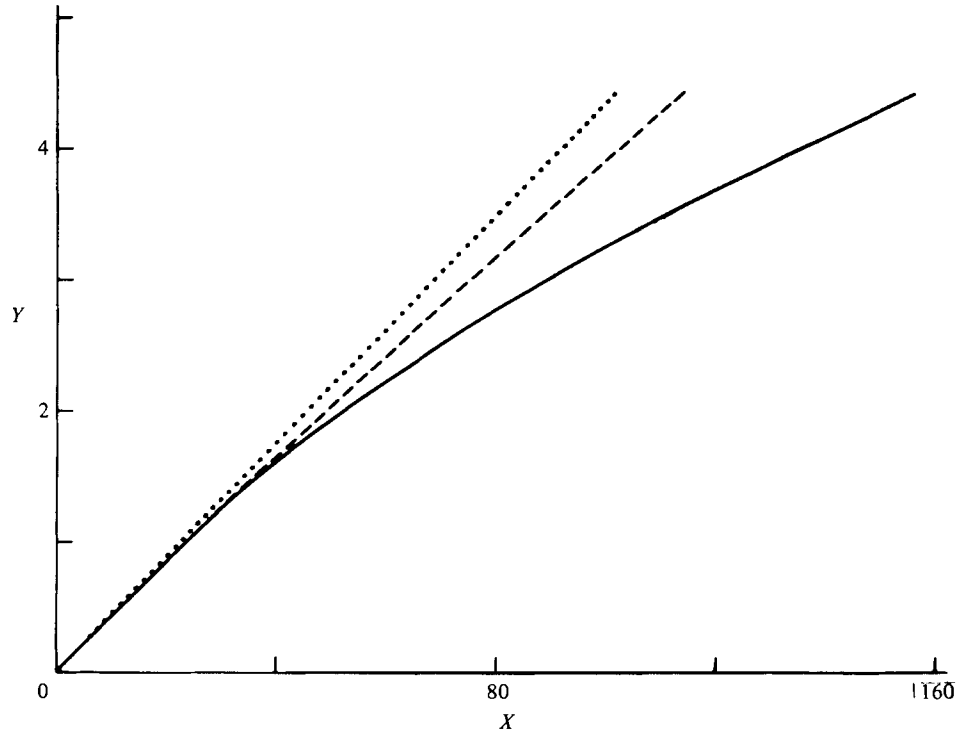

FIGURE 4. Values of the total flow generated by F_0. $X = F_0/\nu^2\rho$, $Y = 2\pi\psi_m/\nu a$, where ψ_m is the maximum value of ψ. ...., linear theory; ---, third-order approximation; ——, numerical solution.

as R increases from 0 until it reaches a minimum; thence it continuously increases with R.

The vorticity field is azimuthal and in the linear problem within a sphere which is centred at O and has radius $R \simeq 0{\cdot}74$ it is directed in the positive ϕ sense, that is $f < 0$, and in the surrounding region it is directed in the opposite sense. As c decreases (from large values) the spherical core where $f < 0$ is shifted in the direction of the force F_0 and is somewhat squeezed, especially for small c as can easily be seen from the regions enclosed by the broken curves in figures 1–3.

One quantity of particular interest is the total volume flow, that is $2\pi\psi_m$, where ψ_m denotes the maximum value of ψ, generated by the force. Figure 4 shows values of this quantity derived from the linear solution, the third-order approximation and our numerical solution. The numerical solution curve was constructed from the three points corresponding to $F_0/\nu^2\rho$ being 8·65, 34·77 and 156·32. These were obtained from the three values of c (5, 1 and 0·2) for which we solved the problem numerically. We must also note that the series expansions for f, g and F_0 are valid for $c > 0$ but [see equation (37)] in the linear approximation values of $F_0/\nu^2\rho$ exceeding $16\pi \simeq 50{\cdot}3$ are associated with negative values of c. Similarly in the case of the third-order approximation c takes negative values when $F_0/\nu^2\rho > 512\pi/15 \simeq 107{\cdot}2$. (The least value of c for the part of the third-order approximation curve shown in figure 4 is about $-0{\cdot}03$.) Figure 4 and also details of our computations show that the linear solution overestimates ψ_m, though

for values of $F_0/\nu^2\rho$ up to about 20 this overestimate is very small. Even when $F_0/\nu^2\rho$ is 50 the overestimate of ψ_m due to the use of the linear theory is less than 20 %. As expected the third-order solution provides a better approximation to ψ_m than the linear theory and when $F_0/\nu^2\rho$ is 50 this solution predicts a value of ψ_m about 6 % higher than that associated with the curve of the full solution. We believe that the conclusions reached in the last four paragraphs are, in general, independent of the geometry of the problem.

We are grateful to Professor Sir James Lighthill for suggestions concerning the presentation of the material and to Mr D. J. Mullings for some programming assistance.

REFERENCES

Batchelor, G. K. 1967 *Introduction to Fluid Dynamics*. Cambridge University Press.
Blake, J. R. 1971 *Proc. Camb. Phil. Soc.* **70**, 303.
Lamb, H. 1962 *Hydrodynamics*. Cambridge University Press.
Le Bail, R. C. 1972 *J. Comp. Phys.* **9**, 440.
Lighthill, M. J. 1976 *SIAM Review* **18**, 161.
Lighthill, M. J. 1978 *Waves in Fluids*. Cambridge University Press.
Liron, N. & Shahar, R. 1978 *J. Fluid Mech.* **86**, 729.
Sozou, C. 1971 *J. Plasma Phys.* **6**, 331.
Sozou, C. & Pickering, W. M. 1976 *J. Fluid Mech.* **73**, 641.
Sozou, C. & Pickering, W. M. 1977 *J. Fluid Mech.* **80**, 673.
Squire, H. B. 1952 *Phil. Mag.* **43** (7), 942.